medRxiv preprint doi: https://doi.org/10.1101/2020.04.09.20058651; this version posted April 14, 2020. The copyright holder for this preprint (which was not certified by peer review) is the author/funder, who has granted medRxiv a license to display the preprint in perpetuity. It is made available under a CC-BY-NC-ND 4.0 International license .

Scaling diagnostics in times of COVID-19: Rapid prototyping of 3D-printed water circulators for Loop-mediated Isothermal Amplification (LAMP) and detection of SARS-CoV-2 virus

Everardo González-González[1,2], Itzel Montserrat Lara-Mayorga[1,3], Andrés García-Rubio[1,3], Carlos Ezio Garciaméndez-Mijares[1,3], Gilberto Emilio-Guerra-Alvarez[1,3], Germán García-Martínez[1,3], Juan Aguayo[1,3], Yu Shrike Zhang[4], Sergio Omar Martínez-Chapa[3,*], Grissel Trujillo-de Santiago[1,3,*], Mario Moisés Alvarez[1,2*]

[1] Centro de Biotecnología-FEMSA, Tecnologico de Monterrey, CP 64849, Monterrey, Nuevo León, México

[2] Departamento de Bioingeniería, Tecnologico de Monterrey, CP 64849, Monterrey, Nuevo León, México

[3] Departamento de Ingeniería Mecátrónica y Eléctrica, Tecnologico de Monterrey, CP 64849, Monterrey, Nuevo León, México

[4] Division of Engineering in Medicine, Department of Medicine, Brigham and Women's Hospital, Harvard Medical School, Cambridge 02139, MA, USA

*Corresponding authors. E-mails: mario.alvarez@tec.mx; grissel@tec.mx

NOTE: This preprint reports new research that has not been certified by peer review and should not be used to guide clinical practice.

medRxiv preprint doi: https://doi.org/10.1101/2020.04.09.20058651; this version posted April 14, 2020. The copyright holder for this preprint (which was not certified by peer review) is the author/funder, who has granted medRxiv a license to display the preprint in perpetuity. It is made available under a CC-BY-NC-ND 4.0 International license .

Abstract

By the first week of April 2020, more than 1,500,000 positive cases of COVID-19 and more than 50,000 deaths had been officially reported worldwide. While developed countries such as the USA, Italy, England, France, Spain, and Germany struggle to mitigate the propagation of SARS-CoV-2, the COVID-19 pandemic arrived in Latin America, India, and Africa—territories in which the mounted infrastructure for diagnosis is greatly underdeveloped. An actual epidemic emergency does not provide the required timeframe for testing new diagnostic strategies; therefore, the first line of response must be based on commercially and readily available resources. Here, we demonstrate the combined use of a three-dimensional (3D)-printed incubation chamber for commercial Eppendorf PCR tubes, and a colorimetric embodiment of a loop-mediated isothermal amplification (LAMP) reaction scheme for the detection of SARS-CoV-2 nucleic acids. We used this strategy to detect and amplify SARS-CoV-2 DNA sequences using a set of in-house designed initiators that target regions encoding the N protein. We were able to detect and amplify SARS-CoV-2 nucleic acids in the range of ~625 to 2×10^5 DNA copies by this straightforward method. The accuracy and simplicity of this diagnostics strategy may provide a cost-efficient and reliable alternative for use during the COVID-19 pandemics, particularly in underdeveloped regions were the availability of RT-qPCR instruments may be limited. Moreover, the portability, ease of use, and reproducibility of this strategy make it a reliable alternative for deployment of point-of-care SARS-CoV-2 detection efforts during the pandemics.

Key words: LAMP, point-of-care, SARS-CoV-2, COVID-19, diagnostic, portable, isothermal nucleic acid amplification

Introduction

By the end of the first week of April 2020, more than one and a half million positive cases of COVID-19 were officially reported across the globe[1]. Even developed countries, such

medRxiv preprint doi: https://doi.org/10.1101/2020.04.09.20058651; this version posted April 14, 2020. The copyright holder for this preprint (which was not certified by peer review) is the author/funder, who has granted medRxiv a license to display the preprint in perpetuity. It is made available under a CC-BY-NC-ND 4.0 International license .

as the USA, England, France, and Germany, are struggling to mitigate the propagation of SARS-CoV-2 by implementing social distancing and widespread testing. Less developed regions, such as Latin America, India, and Africa, are now experiencing the arrival of COVID-19, but these—territories are woefully lacking in the finances or the mounted infrastructure for diagnosis of this pandemic infection. Rapid and massive testing of thousands of possibly infected subjects has been an important component of the strategy of the countries that are effectively mitigating the spreading of COVID-19 among their populations (i.e., China[2], South Korea [3], and Singapore [4]). By comparison, developing countries with high demographic densities, such as México [5], India [6], or Brazil [7], may not be able to implement a sufficient number of centralized laboratories for rapid large-scale testing for COVID-19.

Many methodologies have been proposed recently to deliver cost-effective diagnosis (i.e., those based on immunoassays [8–11] or specific gene hybridization assisted by CRISPR-Cas systems [12–14]). While immunoassays are an accurate and efficacious tool for assessing the extent of the infection for epidemiological studies [15], their usefulness is limited to the identification of infected subjects during early phases of infection [11,16], a critical period for infectiveness. For instance, experimental evidence collected from a small number of COVID-19 patients (9 subjects) showed that 100% of them produced specific immunoglobulins G (IgGs) for SARS-CoV-2 within two weeks of infection, but only 50% of them did during the first week post infection [17].

Nucleic acid amplification continues to be the gold standard for the detection of viral diseases in the early stages [18–22], and very small viral loads present in symptomatic or

medRxiv preprint doi: https://doi.org/10.1101/2020.04.09.20058651; this version posted April 14, 2020. The copyright holder for this preprint (which was not certified by peer review) is the author/funder, who has granted medRxiv a license to display the preprint in perpetuity. It is made available under a CC-BY-NC-ND 4.0 International license .

asymptomatic patients can be reliably detected using amplification based technics, such as PCR[23–25], RPA[26], and LAMP[27–29].

During the last two pandemic events with influenza A/H1N1/2009 and COVID-19, the Centers for Disease Control (CDC) and the World Health Organization (WHO) recommended real-time quantitative PCR (RT-qPCR) methods as the gold standard for official detection of positive cases[16,30]. However, the reliance on RT-qPCR often leads to dependence on centralized laboratory facilities for testing [16,30–33]. To resolve this drawback, isothermal amplification reaction schemes (i.e., loop-mediated isothermal amplification (LAMP) and recombinase polymerase amplification (RPA)) have been proposed as alternatives to PCR-based methods and devices for point-of-care settings [32,34,35]. The urgency of using reliable molecular-based POC methods for massive diagnostic during epidemiological emergencies has become even more evident during the current COVID-19 pandemics [30,36,37].

In these times of COVID-19 [38], scientists and philanthropists around the globe have worked expeditiously on the development of rapid and portable diagnostics for SARS-CoV-2. Several reports have demonstrated the use of colorimetric LAMP-based methods for diagnosis of pandemic COVID-19 [39–44]. Some of these reports (currently available as preprints) use phenol red, a well-known pH indicator, to assist in the visual discrimination between positive and negative samples [39,40].

In this study, we demonstrate the use of a simple embodiment of a colorimetric Loop-mediated Isothermal amplification (LAMP) protocol for the detection and amplification of synthetic samples of SARS-CoV-2, the causal viral agent of COVID-D. In this LAMP-based strategy, also assisted by the use of phenol red, sample incubation is greatly

medRxiv preprint doi: https://doi.org/10.1101/2020.04.09.20058651; this version posted April 14, 2020. The copyright holder for this preprint (which was not certified by peer review) is the author/funder, who has granted medRxiv a license to display the preprint in perpetuity. It is made available under a CC-BY-NC-ND 4.0 International license .

facilitated by the use of a three-dimensional (3D)-printed incubator connected to a conventional water circulator, while discrimination between positive and negative samples is achieved by visual inspection. We quantitatively analyze differences in color between positive and negative samples using color decomposition and analysis in the color CIELab space[45]. Moreover, we compare the sensibility of this LAMP colorimetric method versus PCR protocols. This simple strategy is potentially adequate for the fast deployment of diagnostic efforts in the context of COVID-19 pandemics.

Materials and Methods

Equipment specifications: We ran several hundred amplification experiments using a colorimetric LAMP method in a 3D-printed incubation chamber designed in house and connected to a conventional water circulator (Figure 1). The design and all dimensional specifications of this chamber have been made available in Supplementary Information (Figure S1,S2; Supplementary File S1). In the experiments reported here, we used a chamber with dimensions of 20 × 5 × 15 cm^3 and a weight of 0.4 kg (without water). A conventional water circulator (WVR, PA, USA), was used to circulate hot water (set point value at 76 ºC) through the 3D-printed chamber for incubation of the Eppendorf PCR tubes (0.2 mL). In this first chamber prototype, twelve amplification reactions can be run in parallel. This concept design is amenable for fabrication in any STL-3D printing platform and may be scaled up to accommodate a larger number of tubes.

We used a blueGel electrophoresis unit, powered by 120 AC volts, to validate the LAMP amplification using gel electrophoresis. Photo-documentation was done using a smartphone camera. We also used a Synergy HT microplate reader (BioTek Instruments,

medRxiv preprint doi: https://doi.org/10.1101/2020.04.09.20058651; this version posted April 14, 2020. The copyright holder for this preprint (which was not certified by peer review) is the author/funder, who has granted medRxiv a license to display the preprint in perpetuity. It is made available under a CC-BY-NC-ND 4.0 International license .

VT, USA) to detect the fluorescence induced by an intercalating reagent in positive samples from the PCR reactions.

Validation DNA templates: We used plasmids containing the complete N gene from 2019-nCoV, SARS, and MERS as positive controls, with a concentration of 200,000 copies/µL (Integrated DNA Technologies, IA, USA).

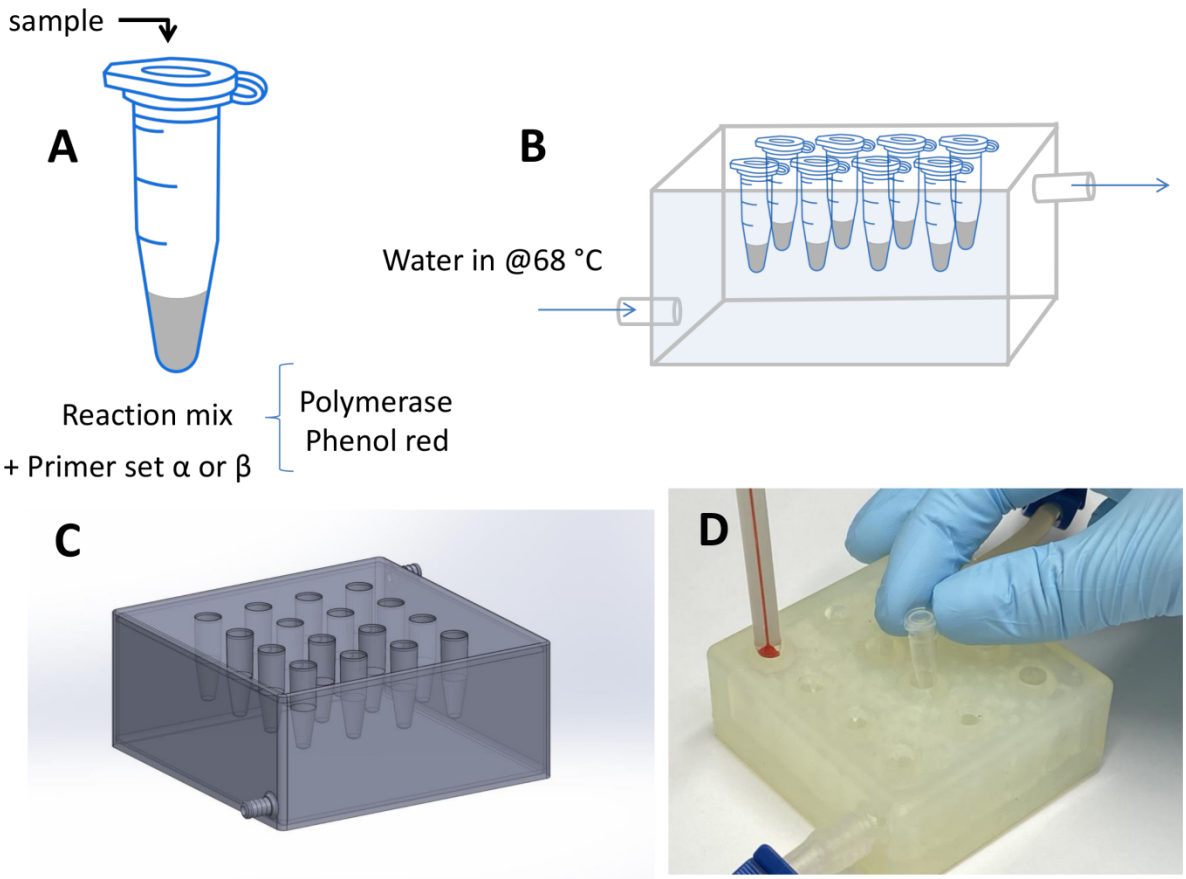

Figure 1. Experimental setup. (A) Commercial 200 microliter Eppendorf PCR tubes, and (B) a 3D-printed incubator were used in amplification experiments of samples containing synthetic SARS-CoV-2 nucleic acid material. (C) 3D CAD model of the LAMP reaction incubator. (D) Actual image of the Eppendorf tube incubator connected to a conventional water circulator.

medRxiv preprint doi: https://doi.org/10.1101/2020.04.09.20058651; this version posted April 14, 2020. The copyright holder for this preprint (which was not certified by peer review) is the author/funder, who has granted medRxiv a license to display the preprint in perpetuity. It is made available under a CC-BY-NC-ND 4.0 International license .

Samples containing different concentrations of synthetic nucleic acids of SARS-CoV-2 were prepared by successive dilutions from stocks (from 2×10^5 copies to 65 copies). We used a plasmid that contained the gene GP from EBOV as a negative control. The production of this EBOV genetic material has been documented elsewhere by our group [23].

Amplification mix: We used WarmStart® Colorimetric LAMP 2× Master Mix (DNA & RNA) from New England Biolabs (MA, USA), and followed the recommended protocol: 12.5 μL Readymix, 1.6 μM FIP primer, 1.6 μM BIP primer, 0.2 μM F3 primer, 0.2 μM B3 primer, 0.4 μM LF primer, 0.4 μM LB primer, 1μL DNA template (~ 625 to 2×10^5 DNA copies), 1.25 μL EvaGreen® Dye from Biotium (CA, USA), and nuclease-free water to a final volume of reaction 25 μL. This commercial mix contains phenol red as a pH indicator for revealing the shift of pH during LAMP amplification across the threshold of pH=6.8.

Primers used: Two different sets of LAMP primers, referred to here as α and β, were designed in house using the LAMP primer design software Primer Explorer V5 (http://primerexplorer.jp/ lampv5e/index.html). These primers were based on the analysis of alignments of the SARS-Co2 N gene sequences using the software Geneious (New Zealand), downloaded from https://www.ncbi.nlm.nih.gov/genbank/sars-cov-2-seqs/#nucleotide-sequences.

Each set, containing six LAMP primers, were used to target two different regions of the sequence of the SARS-Co2 N gene. In addition, for comparison purposes, we conducted PCR amplification experiments using the primer sets recommended by the CDC for the standard diagnostics of COVID-19 (i.e., N1, N2, and N3 assays) using RT-qPCR. The

medRxiv preprint doi: https://doi.org/10.1101/2020.04.09.20058651; this version posted April 14, 2020. The copyright holder for this preprint (which was not certified by peer review) is the author/funder, who has granted medRxiv a license to display the preprint in perpetuity. It is made available under a CC-BY-NC-ND 4.0 International license .

sequences of our LAMP primers are presented in Table 1. The sequences of the PCR primers (N1–N3) have been reported elsewhere[24,46].

Amplification protocols: For all LAMP experiments, we performed isothermal heating for 30 or 60 min. In our experiments, we tested three different temperatures: 50, 60, and 65 ºC.

Table 1. Primer sequences used in LAMP amplification experiments. Two different sets of primers were used, directed at the RNA sequence encoding the N sequence of the SARS-CoV-2.

Set	**Description**	**Primers Sequence (5'>3')**
Primer set α	2019-nCoV 1-F3	TGGACCCCAAAATCAGCG
	2019-nCoV 1-B3	GCCTTGTCCTCGAGGGAAT
	2019-nCoV 1-FIP	CCACTGCGTTCTCCATTCTGGTAAATGCACCCCGCATTACG
	2019-nCoV 1-BIP	CGCGATCAAAACAACGTCGGCCCTTGCCATGTTGAGTGAGA
	2019-nCoV 1-LF	TGAATCTGAGGGTCCACCAA
	2019-nCoV 1-LB	TTACCCAATAATACTGCGTCTTGGT
Primer set β	2019-nCoV 2-F3	CCAGAATGGAGAACGCAGTG
	2019-nCoV 2-B3	CCGTCACCACCACGAATT
	2019-nCoV 2-FIP	AGCGGTGAACCAAGACGCAGGGCGCGATCAAAACAACG
	2019-nCoV 2-BIP	AATTCCCTCGAGGACAAGGCGAGCTCTTCGGTAGTAGCCAA
	2019-nCoV 2-LF	TTATTGGGTAAACCTTGGGGC
	2019-nCoV 2-LB	TAACACCAATAGCAGTCCAGATGA

Documentation of LAMP products: We analyzed 10 μL of each LAMP reaction in a blueGel unit, a portable electrophoresis unit sold by MiniPCR from Amplyus (MA, USA). This is a compact electrophoresis unit (23 × 10 × 7 cm) that weighs 350 g. In these experiments, we analyzed 10 μL of the LAMP product using 1.2 % agarose electrophoresis

medRxiv preprint doi: https://doi.org/10.1101/2020.04.09.20058651; this version posted April 14, 2020. The copyright holder for this preprint (which was not certified by peer review) is the author/funder, who has granted medRxiv a license to display the preprint in perpetuity. It is made available under a CC-BY-NC-ND 4.0 International license .

tris-borate-EDTA buffer (TBE). We used the Quick-Load Purple 2-Log DNA Ladder (NEB, MA, USA) as a molecular weight marker. Gels were dyed with Gel-Green from Biotium (CA, USA) using a 1:10,000 dilution, and a current of 48 V was supplied by the blueGel built-in power supply (AC 100–240V, 50–60Hz).

As an alternative method for detection and reading of the amplification product, we evaluated the amplification products by detecting the fluorescence emitted by a DNA-intercalating agent, the EvaGreen® Dye from Biotium (CA, USA), in a Synergy HT microplate reader (BioTek Instruments, VT, USA). Briefly, 25 μL of the LAMP reaction was placed in separate wells of a 96-well plate following completion of the LAMP incubation. A 125 μL volume of nuclease-free water was added to each well for a final sample volume of 150 μL and the samples were well-mixed by pipetting. These experiments were run in triplicate. The following conditions were used in the microplate reader: excitation of 485/20, emission of 528/20, gain of 75. Fluorescence readings were done from the top at room temperature.

Color determination by image analysis: We also photographically documented and analyzed the progression of color changes in the positive and negative SARS-CoV-2 synthetic samples during the LAMP reaction time (i.e., from 0 to 50 min). For that purpose, Eppendorf PCR tubes containing LAMP samples were photographed using a smartphone (iPhone, from Apple, USA). We used an application for IOS (Color Companion, freely available at Apple store) to determine the components of color of each LAMP sample in the CIELab color space. Color differences between the positive samples and negative controls were calculated as distances in the CIELab coordinate system according to the following formula:

medRxiv preprint doi: https://doi.org/10.1101/2020.04.09.20058651; this version posted April 14, 2020. The copyright holder for this preprint (which was not certified by peer review) is the author/funder, who has granted medRxiv a license to display the preprint in perpetuity. It is made available under a CC-BY-NC-ND 4.0 International license .

$$\text{Color Distance}_{\text{sample-negative}} = \text{SQRT}\ [(L_{sample}-L_{negative})^2 + (a_{sample}-a_{negative})^2 + (b_{sample}-b_{negative})^2]$$

Here L, a, and b are the color components of the sample or the negative control in the CIELab color space (Supplementary Figure 4).

Results and Discussion

Rationale

We have developed a simple diagnostic method for the detection of SARS-CoV-2, the causal agent of COVID-19. The rationale underlying this strategy is centered on achieving the simplest possible integration of easily available reagents, materials, and fabrication techniques to facilitate fast and massive implementation during the current COVID-19 pandemics in low- or middle-income regions.

This method is based on the amplification of the genetic material of SARS-CoV-2 using a loop-mediated isothermal amplification (LAMP). The amplification is conducted using a commercial reaction mix in commercial and widely available 200 µL Eppendorf PCR tubes. Moreover, we have designed and fabricated a simple 3D-printed chamber (Figure 1) for incubation of the Eppendorf tubes and to enable LAMP at high temperatures (50–65 ºC) and extended times (up to 1 h). We show that this incubation chamber, when connected to a conventional water recirculator, enables the successful amplification of positive samples (i.e., samples containing SARS-CoV-2 nucleic acids).

This incubation chamber is one of the key elements that enable rapid and widespread implementation of this diagnostic method at low cost. This 3D-printed incubator can be rapidly printed using standard SLA printers widely available in markets worldwide.

medRxiv preprint doi: https://doi.org/10.1101/2020.04.09.20058651; this version posted April 14, 2020. The copyright holder for this preprint (which was not certified by peer review) is the author/funder, who has granted medRxiv a license to display the preprint in perpetuity. It is made available under a CC-BY-NC-ND 4.0 International license .

Standard 3D-printing resins can be used. The availability of the original AutoCAD files (included here as supplemental material) enables fast modification/optimization of the design for accommodation of a larger number of samples or larger or smaller tubes, adaptation to any available hoses (tubing), and possible incorporation of an on-line color reading system. Indeed, all this is consistent with the main rationale of our proposed diagnostic strategy for pandemic COVID-19: To enabling a fast and feasible response using widespread, distributed, and scalable diagnostics fabricated with widely available resources.

In the following section, we briefly discuss the mechanisms of amplification and visual discrimination between positive and negative samples.

Colorimetric LAMP amplification

The presence of phenol red within the LAMP reaction mix allows for naked-eye discrimination between positive and negative samples. The reaction mix is coupled with the pH color transition of phenol red, a widely used pH indicator, which shifts in color from red to yellow at pH 6.8. During LAMP amplification, the pH of the reaction mix continuously evolves from neutrality to acidic values as protons are produced [27,47]. The mechanism of production of hydrogen ions (H^+) during amplification in weakly buffered solutions has been described [47]. DNA polymerases incorporate a deoxynucleoside triphosphate into the nascent DNA chain. During this chemical event, a pyrophosphate moiety and a hydrogen ion are released as byproducts (Figure 2 A). This release of hydrogen ions is quantitative, according to the reaction scheme illustrated in Figure 2. The caudal of H^+ is high, since it is quantitatively proportional to the number of newly integrated dNTPs. In fact, the

medRxiv preprint doi: https://doi.org/10.1101/2020.04.09.20058651; this version posted April 14, 2020. The copyright holder for this preprint (which was not certified by peer review) is the author/funder, who has granted medRxiv a license to display the preprint in perpetuity. It is made available under a CC-BY-NC-ND 4.0 International license .

quantitative production of H^+ is the basis of previously reported detection methods, such as the semiconductor sequencing technology operating in Ion Torrent sequencers[48].

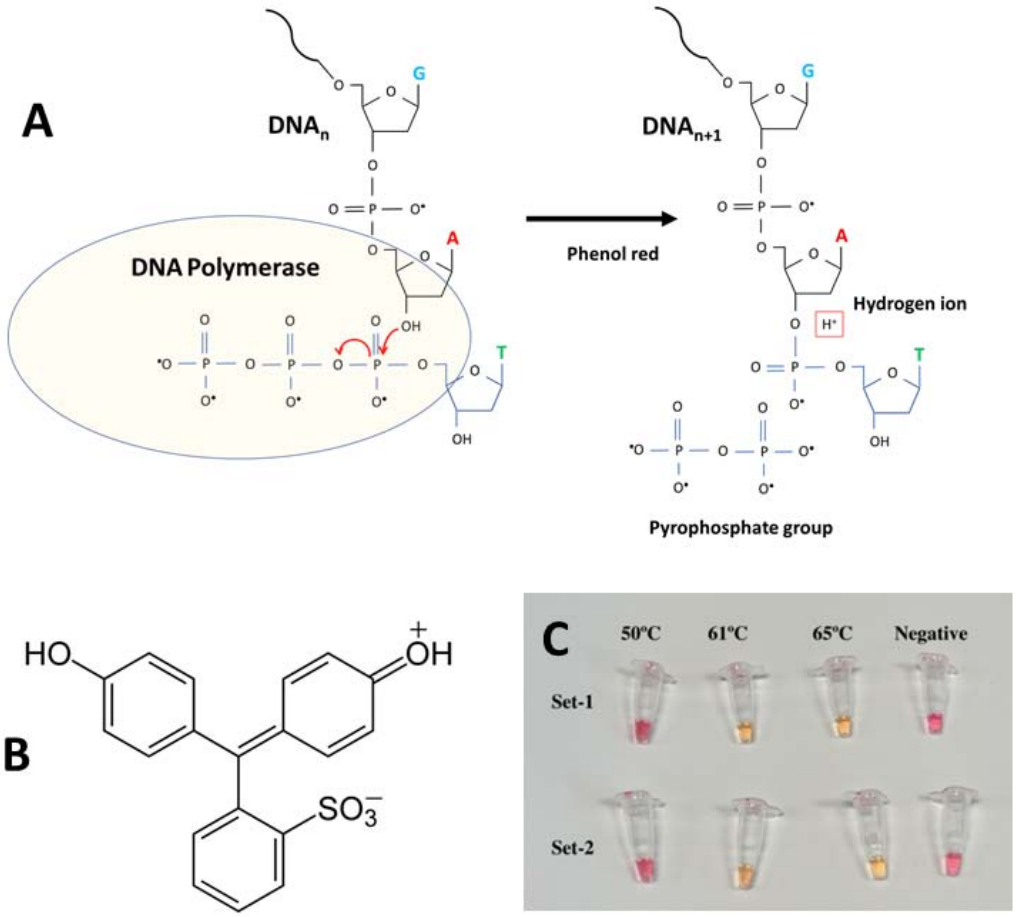

Figure 2. **Initiators and pH indicator for SARS-Co2 detection using a colorimetric LAMP method**. (A) LAMP reaction scheme. (B) Chemical structure of phenol red. (C) Two different sets of LAMP primers were used for successfully targeting a gene sequence encoding the SARS-Co2 N protein. Successful targeting and amplification is clearly evident to the naked eye: positive samples shift from red to yellow.

In the initially neutral and weakly buffered reaction mixes, the production of H^+ during LAMP amplification progressively and rapidly shifts the pH across the threshold of phenol red (Figure 2B).

medRxiv preprint doi: https://doi.org/10.1101/2020.04.09.20058651; this version posted April 14, 2020. The copyright holder for this preprint (which was not certified by peer review) is the author/funder, who has granted medRxiv a license to display the preprint in perpetuity. It is made available under a CC-BY-NC-ND 4.0 International license .

Moreover, the pH shift is clearly evident to the naked eye, thereby freeing the user from reliance on spectrophotometric instruments and facilitating simple implementation during emergencies (Figure 2C). Images in Figure 2C show representative colors of the amplification reaction mixes contained in Eppendorf PCR tubes after incubation for 30 min. Three different incubation temperatures were tested (50, 60, and 65 ºC) and two different sets of LAMP-primers (α and β) were used.

Both sets of primers performed equivalently, at least based on visual inspection, in the three temperature conditions tested. Discrimination between positive and negative controls is possible using only the naked eye to discern the reaction products from amplifications conducted at 60 and 65 ºC. No or negligible amplification was evident at 50 ºC or in the control group.

Furthermore, we were able to successfully discriminate between positive and negative samples using LAMP reaction mix already added with primers and kept at room temperature for 48 h or at 4 °C for 72 hours (Figure S3). The stability of the reaction, the isothermal nature of the amplification process, and its independence from specialized equipment greatly simplifies the logistic of implementation of this diagnostic method outside centralized labs.

Analysis of sensitivity

We conducted a series of experiments to assess the sensitivity of the LAMP reactions in the 3D-printed incubation chamber using the two sets of primers (α and β; Table 1). The amplification proceeds with sufficient quality to also allow proper visualization of the amplification products in electrophoresis gels, even at low nucleic acid concentrations. We observed that amplification proceeded successfully in a wide range of viral loads, from 625

medRxiv preprint doi: https://doi.org/10.1101/2020.04.09.20058651; this version posted April 14, 2020. The copyright holder for this preprint (which was not certified by peer review) is the author/funder, who has granted medRxiv a license to display the preprint in perpetuity. It is made available under a CC-BY-NC-ND 4.0 International license .

to 5×10^5 copies in experiments using synthetic SARS-CoV-2 nucleic acid material (Figure 3A).

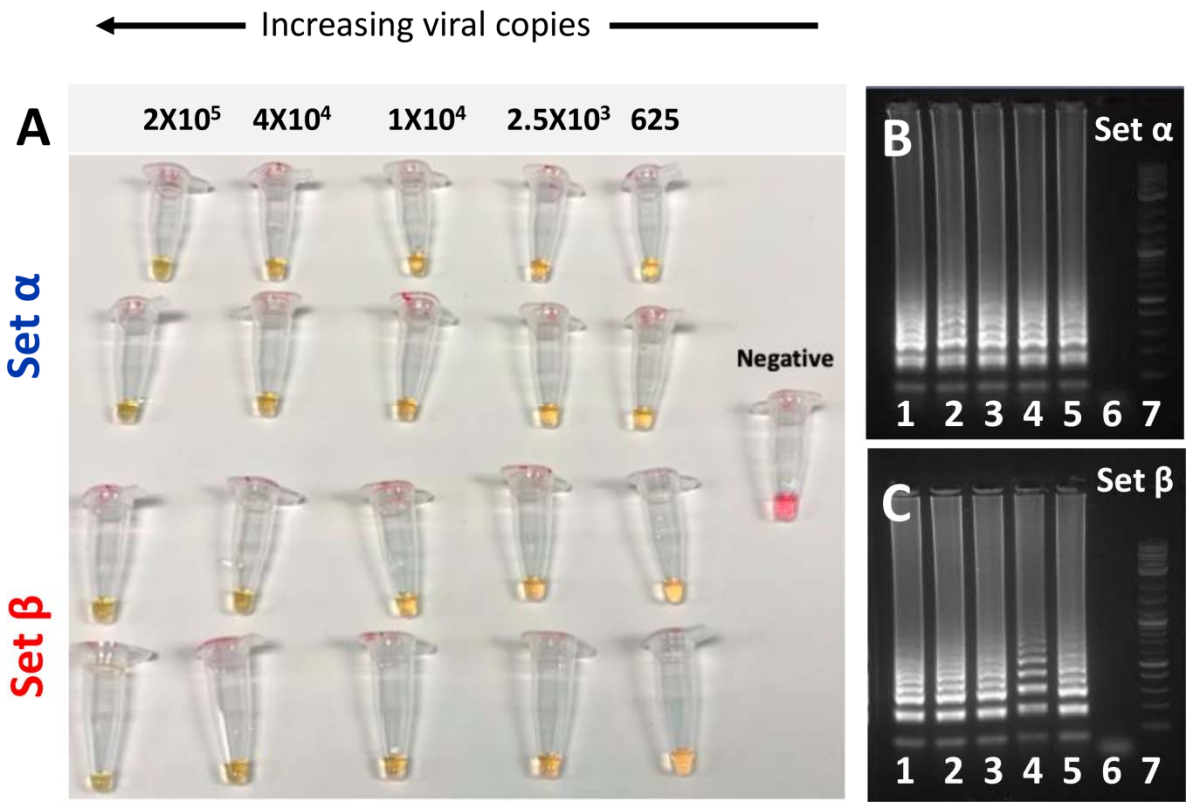

Figure 3. **Two different sets of LAMP-primers were used for successfully targeting of a gene sequence encoding the SARS-Co2 N protein**. (A) LAMP primer sets α and β both enable the amplification of synthetic samples of SARS-CoV-2 nucleic acids in a wide range of template concentrations, from 625 to 2.0×10^5 DNA copies of SARS-CoV-2 when incubated for 50 minutes at a temperature range from 60 to 65 ºC. (B,C) Agarose gel electrophoresis of DNA amplification products generated by targeting two different regions of the sequence coding for SARS-Co2 N protein. Two different primer sets were used: (B) primer set α, and (C) primer set β. The initial template amount was gradually decreased from left to right: 2.0×10^5 DNA copies (lane 1), 4.0×10^4 copies, (lane 2), 1.0×10^4 copies (lane 3), 2.5×10^3 copies (lane 4), 625 copies (lane 5), negative control (lane 6), and molecular weight ladder (lane 7).

medRxiv preprint doi: https://doi.org/10.1101/2020.04.09.20058651; this version posted April 14, 2020. The copyright holder for this preprint (which was not certified by peer review) is the author/funder, who has granted medRxiv a license to display the preprint in perpetuity. It is made available under a CC-BY-NC-ND 4.0 International license .

We clearly observed amplification in samples containing as few as 625 viral copies after incubation times of 5 min at 65 ºC. If we put this range into a proper clinical context, the actual viral load of COVID-19 in nasal swabs from patients has been estimated to fall within the range of 10^5 to 10^6 viral copies per mL [49]. Discrimination between positive and negative samples (controls) can be clearly established by the naked eye in all reactions incubated for 50 min, regardless of the number of viral copies present. In addition, we did not observe any non-specific amplification in negative samples (i.e., containing synthetic genetic material form EBOV) incubated for 50 min at 65 ºC. Indeed, the identification and amplification of SARS-CoV-2 synthetic material is feasible in samples that contained ~62.5 viral copies using this LAMP strategy (Figure S3) and incubation times of 50–60 min.

We corroborated the amplification by visualizing LAMP products with gel electrophoresis for the different viral loads tested. Figures 3B,C show agarose gels of the amplification products of each one of the LAMP experiments, where two different sets of primers (α and β) were used to amplify the same range of concentrations of template (from 625 to 2×10^5 synthetic viral copies). We were able to generate a visible array of bands of amplification products, a typical signature of LAMP, for both LAMP primer sets and across the whole range of synthetic viral loads. Indeed, both primer sets rendered similar amplification profiles.

In summary, using the primers and methods described here, we were able to consistently detect the presence of SARS-CoV-2 synthetic nucleic acids. We have used a simple 3D-printed incubator, connected to a water circulator, to conduct LAMP. We show that, after only 30 min of incubation, samples containing a viral load in the range of 10^4 to 10^5 copies could be clearly discriminated from negative samples by visual inspection with the naked eye (Figure 2C). Samples with a lower viral load were clearly discriminated when the

medRxiv preprint doi: https://doi.org/10.1101/2020.04.09.20058651; this version posted April 14, 2020. The copyright holder for this preprint (which was not certified by peer review) is the author/funder, who has granted medRxiv a license to display the preprint in perpetuity. It is made available under a CC-BY-NC-ND 4.0 International license .

LAMP reaction was incubated for 50 min. Incubation periods of up to 1 h at 68 ºC did not induced false positives and were able to amplify as few as ~62 copies of SARS-CoV-2 synthetic genetic material. These results are consistent with those of other reports in which colorimetric LAMP, assisted by phenol red, has been used to amplify SARS-COV-2 genetic material [39,40].

We observe 0 false positive cases in experiments where synthetic samples containing EBOV genetic material were incubated at 65 ºC for 1 h.

In the current context of the COVID-19 pandemics, the importance of communicating this result does not reside in its novelty but in its practicality. Some cost considerations follow. While the market value of a traditional RT-qPCR apparatus (the current gold standard for COVID-19 diagnostics) is in the range of 10,000 to 40,000 USD, a 3D-printed incubator, such as the one described here (Figure S1,S2; Supplementary file S1), could be fabricated for under 200 USD at any 3D printer shop. This difference is significant, especially during an epidemic or pandemic crisis when rational investment of resources is critical. While the quantitative capabilities of testing using an RT-qPCR platform are undisputable, the capacity of many countries to rapidly, effectively, and massively establish diagnostic centers based on RT-qPCR is questionable. The current pandemic scenarios experienced in the USA, Italy, France, and Spain, among others, have crudely demonstrated that centralized labs are not an ideal solution during emergencies. Portable diagnostic systems may provide a vital flexibility and speed of response that RT-qPCR platforms cannot deliver.

medRxiv preprint doi: https://doi.org/10.1101/2020.04.09.20058651; this version posted April 14, 2020. The copyright holder for this preprint (which was not certified by peer review) is the author/funder, who has granted medRxiv a license to display the preprint in perpetuity. It is made available under a CC-BY-NC-ND 4.0 International license .

Feasibility of real-time quantification

Here, we further illustrate the deterministic and quantitative dependence between the concentration of the amplification product and the color signal produced during this colorimetric LAMP reaction. For this purpose, we simulated real-time amplification experiments by conducting a series of amplification reactions using initial amounts of 625, 1×10^4, and 2×10^5 copies of synthetic SARS-CoV-2 genetic material in our 3D-printed incubator.

We extracted samples from the incubator after 0, 10, 20, 30, 40, and 50 min of incubation at 65 ºC. The color of these samples was documented as images captured using a smart phone (iPhone 7) against a white background (Figure 4A). The images were analyzed using the free access application Color Companion® for the iPhone or iPad. Briefly, color images were decomposed into their CIELab space components. In the CIELab color space, each color can be represented as a point in a 3D-space, defined by the values **L**, **a**, and **b** [45]. In this coordinate system, **L** is the luminosity (which ranges from 0 to +100), **a** is the blue-yellow axis (which ranges from -50 to 50), and **b** is the green-red axis (which ranges from -50 to 50) (Figure S4).

The difference between two colors can be quantitatively represented as the distance between the two points that those colors represent in the CIELab coordinate system. For the colorimetric LAMP reaction mixture used in our experiments, the spectrum of possible colors evolves from red (for negative controls and negative samples) to yellow (for positive samples). Conveniently, the full range of colors for samples and controls can be represented in the red and yellow quadrant defined by L [0,50], a [0,50], and b [0,50]. For instance, the difference between the color of a sample (at any time of the reaction) and the color of the

medRxiv preprint doi: https://doi.org/10.1101/2020.04.09.20058651; this version posted April 14, 2020. The copyright holder for this preprint (which was not certified by peer review) is the author/funder, who has granted medRxiv a license to display the preprint in perpetuity. It is made available under a CC-BY-NC-ND 4.0 International license .

negative control (red; L=53.72 ± 0.581, a=38.86 ± 2.916, and b=11.86 ± 0.961) can be calculated in the CIELab space.

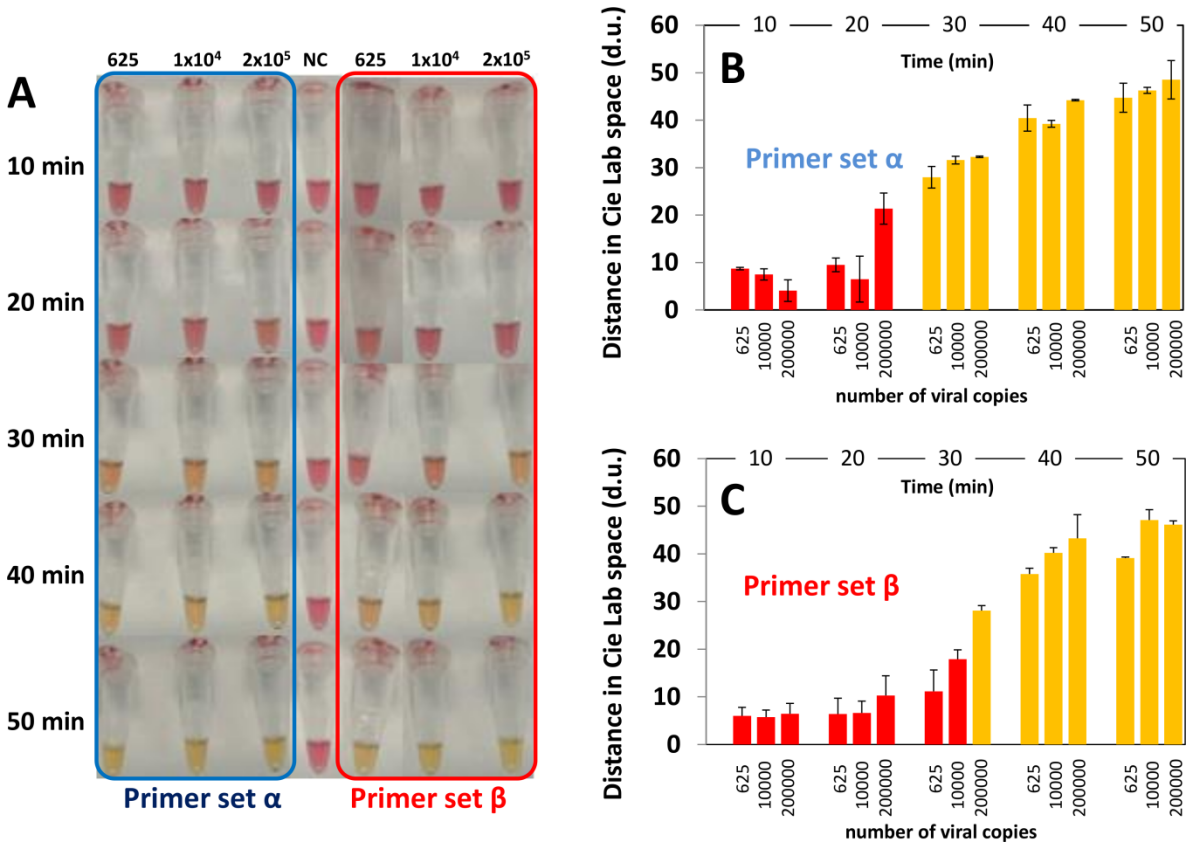

Figure 4. Evaluation of the sensitivity of the combined use of a colorimetric LAMP method assisted by the use of phenol red. (A) Sensitivity trials using different concentrations of the template (positive control) and two different primers sets: α (indicated in blue) and β (indicated in red). Photographs of the Eppendorf PCR tubes containing positive samples and negative controls were acquired using a smartphone. (C,D) Distance in the color CIELab space between negative controls (red) and samples containing different concentrations of SARS-CoV-2 nucleic acid material (i.e., 625, 10000, and 200000 synthetic copies) analyzed after different times of incubation (i.e., 10, 20, 30, 40, and 50 minutes) at 65 °C. The analysis of color distances is presented for amplifications conducted using primer set (B) α and (C) β.

We determined the distance in the CIELab space between the color of samples taken at different incubation times that contained SARS-CoV-2 genetic material and negative

medRxiv preprint doi: https://doi.org/10.1101/2020.04.09.20058651; this version posted April 14, 2020. The copyright holder for this preprint (which was not certified by peer review) is the author/funder, who has granted medRxiv a license to display the preprint in perpetuity. It is made available under a CC-BY-NC-ND 4.0 International license .

controls (Figure 4B and C). We repeated this calculation for each of the LAMP primer sets that we used, namely primer set α (Figure 4B) and β (Figure 4C).

These results suggest that the color difference between the samples and negative controls is quantifiable. Therefore, color analysis may be implemented to assist the discrimination between positives and negatives. Furthermore, imaging and color analysis techniques may be implemented in this simple colorimetric LAMP diagnostic strategy to render a real-time quantitative Lamp (RT-qLAMP). Alternatively, the progression of the amplification at different times can be monitored by adding an intercalating DNA agent, (i.e., EvaGreen Dye), and measuring fluorescence on time (Figure S5).

Note that the variance coefficients for the control are 1.08, 7.50, and 8.10% for L, a, and b, respectively. These small values suggest robustness and reproducibility in the location of the coordinates of the control point (reference point). Similarly, the variation in color between negative controls and positive samples incubated for 50 min was reproducible and robust (average of 46.60 +/- 4.02 d.u.; variance coefficient of 8.62%).

Finally, we observed differences in the performance of the two LAMP primer sets used in the experiments reported here (Figure 4B and 5).

Our results suggest that primer set α enabled faster amplification in samples with fewer viral copies. Consistently, this primer set yielded positive discrimination in samples with 625 viral copies in 30 min (Figure 4B). The use of primer set β enabled similar differences in color, measured as distances in the CIELAB 3D-space, in 40 min (Figure 4C). These findings suggest that primer set α should be preferred for final-point implementations of this colorimetric LAMP method. Interestingly, primer set β may better serve the purpose of a real-time implementation. While primer set α produced similar trajectories of evolution of color in samples that contained 1.0×10^4 and 2.0×10^5 viral copies (Figure 5A), primer set

medRxiv preprint doi: https://doi.org/10.1101/2020.04.09.20058651; this version posted April 14, 2020. The copyright holder for this preprint (which was not certified by peer review) is the author/funder, who has granted medRxiv a license to display the preprint in perpetuity. It is made available under a CC-BY-NC-ND 4.0 International license .

β was better at discriminating between amplifications produced from different initial viral loads (Figure 5B).

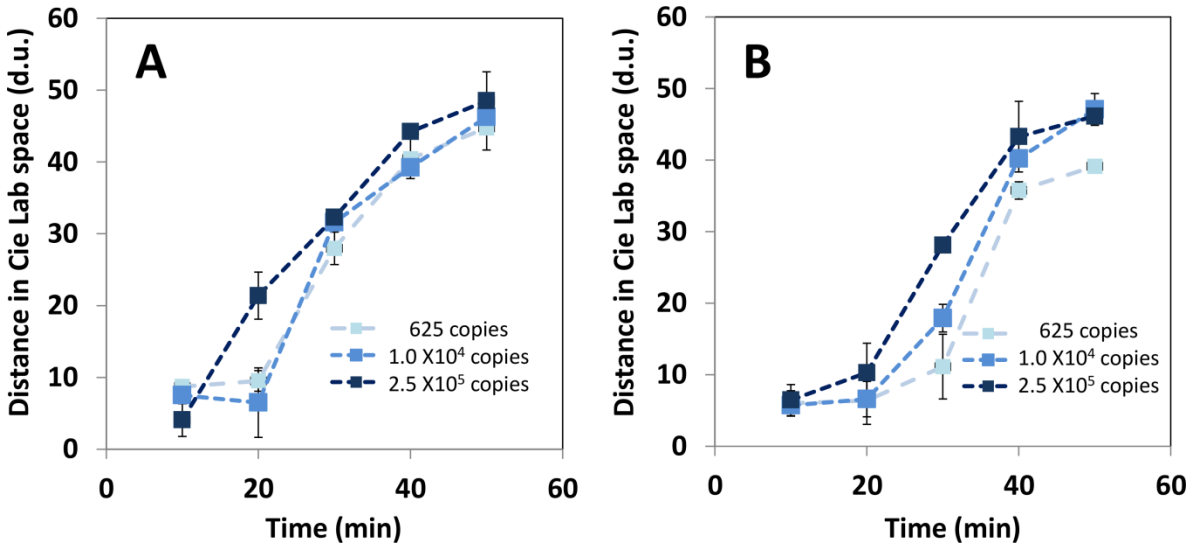

Figure 5. Time progression of the distance in color with respect to negative controls (red color) in the CIELab space for positive SARS-CoV-2 samples containing 625 (light blue, ▫), 1×10^4 (medium blue, ▪), and 2.5×10^6 (dark blue, ■) copies of synthetic of SARS-CoV-2 nucleic acids. Results obtained in experiments using (A) primer set α, and (B) primer set β.

Conclusions

The challenge of point-of-care detection of viral threats is of paramount importance, particularly in underdeveloped regions and in emergency situations (i.e., epidemic outbreaks). In the context of the current COVID-19 pandemic, the availability of testing infrastructure based on RT-qPCR is recognized as a serious challenge around the world. In developing economies (i.e. Latin America, India, and most African countries), the currently available resources for massive COVID-19 testing by RT-qPCR will clearly be insufficient.

medRxiv preprint doi: https://doi.org/10.1101/2020.04.09.20058651; this version posted April 14, 2020. The copyright holder for this preprint (which was not certified by peer review) is the author/funder, who has granted medRxiv a license to display the preprint in perpetuity. It is made available under a CC-BY-NC-ND 4.0 International license .

Even in developed countries, the time to get diagnostic RT-qPCR results from a COVID-19 RT-qPCR test currently ranges from 1 to 5 days. Clearly, the available PCR labs are overburdened with samples, have too few personnel to conduct the tests, are struggling with backlogs on the instrumentation, and face complicated logistics to transport delicate and infective samples while preserving the cold chain.

Here, we have demonstrated that a simple embodiment of a LAMP reaction, assisted by the use of phenol red as a pH indicator and the use of a simple 3D-printed chamber connected to a water circulator, can enable the rapid and highly accurate identification of samples that contain artificial SARS-CoV-2 genetic sequences. Amplification is visually evident, without the need for any additional instrumentation, even at low viral copy numbers. In our experiments with synthetic samples, we observed 100 percent accuracy in samples containing as few as 625 copies of SARS-CoV-2 genetic material.

Validation of these results using real human samples from positive and negative COVID-19 subjects is obviously needed to obtain a full assessment of the potential of this strategy as an alternative to RT-qPCR platforms. However, our results with synthetic samples suggest that this simple strategy may greatly enhance the capabilities for COVID-19 testing in situations where RT-qPCR is not feasible or is unavailable.

Acknowledgments

EGG acknowledges funding from a doctoral scholarship provided by CONACyT (Consejo Nacional de Ciencia y Tecnología, México). GTdS and MMA acknowledge the institutional funding received from Tecnológico de Monterrey (Grant 002EICIS01), and funding provided by CONACyT (Consejo Nacional de Ciencia y Tecnología, México) through grants (SNI 26048, SNI 256730, and Scholarships 635891, 856068, and 814593).

medRxiv preprint doi: https://doi.org/10.1101/2020.04.09.20058651; this version posted April 14, 2020. The copyright holder for this preprint (which was not certified by peer review) is the author/funder, who has granted medRxiv a license to display the preprint in perpetuity. It is made available under a CC-BY-NC-ND 4.0 International license .

Supporting Information

Supporting Information

Figure S1. (A) Actual images, and (B) rendering of the 3D- printed incubation chamber used in the LAMP experiments.

Figure S2. Schematic representation of the chamber (different views) showing its relevant dimensions.

Figure S3. (A) The colorimetric LAMP method described here was able to identify and amplify synthetic SARS-CoV-2 genetic material in samples containing as few as ~62 viral copies. (B) Evaluation of the stability and functionality of the LAMP reaction mix at different storage times and temperatures. The reaction mix, which is formulated with LAMP primers and ready for the addition of nucleic acid extracts, is functional and discriminates between positive and negative samples when stored (i) at room temperature for 48 h or (ii) at 4 °C for 72 h.

Figure S4. (A) Color analysis conducted on positive and negative SARS-CoV-2 samples contained in Eppendorf PCR tubes (yellow inset) using Color Companion, a freely available app from Apple (downloadable at Apple Store, USA). This app identifies the components of color in a specific location of an image (black circle in the yellow inset) in the CIELab, RGB, HSB, or CMYK spaces. The image can be uploaded using e-mail, airdrop, or Whatsapp. (B) Schematic representation of the CIELab space, a color system where any color can be represented in terms of a point and its coordinates in a 3D space, where L is luminosity, a is the axis between green and red, and b is the axis between yellow and red.

Figure S5. (A) The amount of amplification product in LAMP experiments was evaluated by measuring the fluorescence emitted by the amplification product in reactions with an added intercalating agent. Fluorescence readings were conducted in standard 96-well plates and using a conventional plate reader. (A) Fluorescence readings, as measured in a

medRxiv preprint doi: https://doi.org/10.1101/2020.04.09.20058651; this version posted April 14, 2020. The copyright holder for this preprint (which was not certified by peer review) is the author/funder, who has granted medRxiv a license to display the preprint in perpetuity. It is made available under a CC-BY-NC-ND 4.0 International license .

commercial plate reader, for different dilutions of SARS-CoV-2 synthetic DNA templates. Results using two different LAMP primer sets are shown: set α (indicated in blue), and set β (indicated in red).

References

1. Coronavirus Disease (COVID-19) – Statistics and Research - Our World in Data [Internet]. [cited 8 Apr 2020]. Available: https://ourworldindata.org/coronavirus?fbclid=IwAR28tcRVA1rmXsVCrYHcxuHpRXeyO9-uxFJFSG5-lv5gsJgzDxK7eN08i_Y
2. Bedford J, Enria D, Giesecke J, Heymann DL, Ihekweazu C, Kobinger G, et al. COVID-19: towards controlling of a pandemic. The Lancet. Lancet Publishing Group; 2020. pp. 1015–1018. doi:10.1016/S0140-6736(20)30673-5
3. Cohen J, Kupferschmidt K. Countries test tactics in “war” against COVID-19. Science. American Association for the Advancement of Science; 2020;367: 1287–1288. doi:10.1126/science.367.6484.1287
4. Pung R, Chiew CJ, Young BE, Chin S, I-C Chen M, Clapham HE, et al. Articles Investigation of three clusters of COVID-19 in Singapore: implications for surveillance and response measures. Lancet. Elsevier; 2020;19: 1–8. doi:10.1016/S0140-6736(20)30528-6
5. Alvarez MM, Gonzalez-Gonzalez E, Santiago GT. Modeling COVID-19 epidemics in an Excel spreadsheet: Democratizing the access to first-hand accurate predictions of epidemic outbreaks. medRxiv. Cold Spring Harbor Laboratory Press; 2020; 2020.03.23.20041590. doi:10.1101/2020.03.23.20041590
6. Singh R, Adhikari R. Age-structured impact of social distancing on the COVID-19

medRxiv preprint doi: https://doi.org/10.1101/2020.04.09.20058651; this version posted April 14, 2020. The copyright holder for this preprint (which was not certified by peer review) is the author/funder, who has granted medRxiv a license to display the preprint in perpetuity. It is made available under a CC-BY-NC-ND 4.0 International license .

epidemic in India. 2020; Available: http://arxiv.org/abs/2003.12055

7. Bastos SB, Cajueiro DO. Modeling and forecasting the Covid-19 pandemic in Brazil. 2020; Available: http://arxiv.org/abs/2003.14288

8. Yen C-W, de Puig H, Tam JO, Gómez-Márquez J, Bosch I, Hamad-Schifferli K, et al. Multicolored silver nanoparticles for multiplexed disease diagnostics: distinguishing dengue, yellow fever, and Ebola viruses. Lab Chip. The Royal Society of Chemistry; 2015;15: 1638–1641. doi:10.1039/C5LC00055F

9. Mou L, Jiang X. Materials for Microfluidic Immunoassays: A Review. Adv Healthc Mater. Wiley-VCH Verlag; 2017;6: 1601403. doi:10.1002/adhm.201601403

10. Alvarez MM, López-Pacheco F, Aguilar-Yañez JM, Portillo-Lara R, Mendoza-Ochoa GI, García-Echauri S, et al. Specific Recognition of Influenza A/H1N1/2009 Antibodies in Human Serum: A Simple Virus-Free ELISA Method. Jeyaseelan S, editor. PLoS One. Public Library of Science; 2010;5: e10176. doi:10.1371/journal.pone.0010176

11. Zhong L, Chuan J, Gong B, Shuai P, Zhou Y, Zhang Y, et al. Detection of serum IgM and IgG for COVID-19 diagnosis. Sci CHINA Life Sci. Science China Press; 2020; doi:10.1007/S11427-020-1688-9

12. Pardee K, Green AA, Takahashi MK, Braff D, Lambert G, Lee JW, et al. Rapid, Low-Cost Detection of Zika Virus Using Programmable Biomolecular Components. Cell. Cell Press; 2016;165: 1255–1266. doi:10.1016/J.CELL.2016.04.059

13. Broughton JP, Deng X, Yu G, Fasching CL, Streithorst J, Granados A, et al. Rapid Detection of 2019 Novel Coronavirus SARS-CoV-2 Using a CRISPR-based 1 DETECTR Lateral Flow Assay 2 3. doi:10.1101/2020.03.06.20032334

14. Chen JS, Ma E, Harrington LB, Da Costa M, Tian X, Palefsky JM, et al. CRISPR-

medRxiv preprint doi: https://doi.org/10.1101/2020.04.09.20058651; this version posted April 14, 2020. The copyright holder for this preprint (which was not certified by peer review) is the author/funder, who has granted medRxiv a license to display the preprint in perpetuity. It is made available under a CC-BY-NC-ND 4.0 International license .

Cas12a target binding unleashes indiscriminate single-stranded DNase activity. Science (80-). American Association for the Advancement of Science; 2018;360: 436–439. doi:10.1126/science.aar6245

15. Elizondo-Montemayor L, Alvarez MM, Hernández-Torre M, Ugalde-Casas PA, Lam-Franco L, Bustamante-Careaga H, et al. Seroprevalence of antibodies to influenza A/H1N1/2009 among transmission risk groups after the second wave in Mexico, by a virus-free ELISA method. Int J Infect Dis. Elsevier; 2011;15: e781–e786. doi:10.1016/j.ijid.2011.07.002

16. Tang Y-W, Schmitz JE, Persing DH, Stratton CW. The Laboratory Diagnosis of COVID-19 Infection: Current Issues and Challenges. J Clin Microbiol. American Society for Microbiology Journals; 2020; doi:10.1128/JCM.00512-20

17. Wölfel R, Corman VM, Guggemos W, Seilmaier M, Zange S, Müller MA, et al. Virological assessment of hospitalized patients with COVID-2019. Nature. Nature Publishing Group; 2020; 1–10. doi:10.1038/s41586-020-2196-x

18. Mauk MG, Song J, Bau HH, Liu C. Point-of-Care Molecular Test for Zika Infection. Clin Lab Int. NIH Public Access; 2017;41: 25–27. Available: http://www.ncbi.nlm.nih.gov/pubmed/28819345

19. Liao S-C, Peng J, Mauk MG, Awasthi S, Song J, Friedman H, et al. Smart cup: A minimally-instrumented, smartphone-based point-of-care molecular diagnostic device. Sensors Actuators B Chem. Elsevier; 2016;229: 232–238. doi:10.1016/J.SNB.2016.01.073

20. Jansen van Vuren P, Grobbelaar A, Storm N, Conteh O, Konneh K, Kamara A, et al. Comparative Evaluation of the Diagnostic Performance of the Prototype Cepheid GeneXpert Ebola Assay. J Clin Microbiol. American Society for Microbiology;

medRxiv preprint doi: https://doi.org/10.1101/2020.04.09.20058651; this version posted April 14, 2020. The copyright holder for this preprint (which was not certified by peer review) is the author/funder, who has granted medRxiv a license to display the preprint in perpetuity. It is made available under a CC-BY-NC-ND 4.0 International license .

2016;54: 359–67. doi:10.1128/JCM.02724-15

21. Craw P, Balachandran W. Isothermal nucleic acid amplification technologies for point-of-care diagnostics: a critical review. Lab Chip. The Royal Society of Chemistry; 2012;12: 2469. doi:10.1039/c2lc40100b

22. Hsieh K, Patterson AS, Ferguson BS, Plaxco KW, Soh HT. Rapid, sensitive, and quantitative detection of pathogenic DNA at the point of care through microfluidic electrochemical quantitative loop-mediated isothermal amplification. Angew Chem Int Ed Engl. NIH Public Access; 2012;51: 4896–900. doi:10.1002/anie.201109115

23. Gonzá Lez-Gonzá Lez E, Mendoza-Ramos JL, Pedrozaid SC, Cuellar-Monterrubio A, Má Rquez-Ipiña AR, Lira-Serhanid D, et al. Validation of use of the miniPCR thermocycler for Ebola and Zika virus detection. 2019; doi:10.1371/journal.pone.0215642

24. Gonzalez-Gonzalez E, Santiago GT, Lara-Mayorga IM, Martinez-Chapa SO, Alvarez MM. Portable and accurate diagnostics for COVID-19: Combined use of the miniPCR thermocycler and a well-plate reader for SARS-Co2 virus detection. medRxiv. Cold Spring Harbor Laboratory Press; 2020; 2020.04.03.20052860. doi:10.1101/2020.04.03.20052860

25. Lan L, Xu D, Ye G, Xia C, Wang S, Li Y, et al. Positive RT-PCR Test Results in Patients Recovered From COVID-19. JAMA. 2020; doi:10.1001/jama.2020.2783

26. El-Tholoth M, Bau HH, Song J. A Single and Two-Stage, Closed-Tube, Molecular Test for the 2019 Novel Coronavirus (COVID-19) at Home, Clinic, and Points of Entry. ChemRxiv; 2020; doi:10.26434/CHEMRXIV.11860137.V1

27. Kaarj K, Akarapipad P, Yoon JY. Simpler, Faster, and Sensitive Zika Virus Assay Using Smartphone Detection of Loop-mediated Isothermal Amplification on Paper

medRxiv preprint doi: https://doi.org/10.1101/2020.04.09.20058651; this version posted April 14, 2020. The copyright holder for this preprint (which was not certified by peer review) is the author/funder, who has granted medRxiv a license to display the preprint in perpetuity. It is made available under a CC-BY-NC-ND 4.0 International license .

Microfluidic Chips. Sci Rep. Nature Publishing Group; 2018;8: 1–11. doi:10.1038/s41598-018-30797-9

28. Tomita N, Mori Y, Kanda H, Notomi T. Loop-mediated isothermal amplification (LAMP) of gene sequences and simple visual detection of products. Nat Protoc. Nature Publishing Group; 2008;3: 877–882. doi:10.1038/nprot.2008.57

29. Goto M, Honda E, Ogura A, Nomoto A, Hanaki KI. Colorimetric detection of loop-mediated isothermal amplification reaction by using hydroxy naphthol blue. Biotechniques. 2009;46: 167–172. doi:10.2144/000113072

30. Yang T, Wang Y-C, Shen C-F, Cheng C-M. Point-of-Care RNA-Based Diagnostic Device for COVID-19. Diagnostics. MDPI AG; 2020;10: 165. doi:10.3390/diagnostics10030165

31. Kozel TR, Burnham-Marusich AR. Point-of-Care Testing for Infectious Diseases: Past, Present, and Future. J Clin Microbiol. American Society for Microbiology; 2017;55: 2313–2320. doi:10.1128/JCM.00476-17

32. Su W, Gao X, Jiang L, Qin J. Microfluidic platform towards point-of-care diagnostics in infectious diseases. J Chromatogr A. Elsevier; 2015;1377: 13–26. doi:10.1016/J.CHROMA.2014.12.041

33. Drancourt M, Michel-Lepage A, Boyer S, Raoult D. The Point-of-Care Laboratory in Clinical Microbiology. Clin Microbiol Rev. American Society for Microbiology; 2016;29: 429–47. doi:10.1128/CMR.00090-15

34. Jangam SR, Agarwal AK, Sur K, Kelso DM. A point-of-care PCR test for HIV-1 detection in resource-limitedsettings. Biosens Bioelectron. Elsevier; 2013;42: 69–75. doi:10.1016/J.BIOS.2012.10.024

35. Qiu X, Ge S, Gao P, Li K, Yang S, Zhang S, et al. A smartphone-based point-of-care

medRxiv preprint doi: https://doi.org/10.1101/2020.04.09.20058651; this version posted April 14, 2020. The copyright holder for this preprint (which was not certified by peer review) is the author/funder, who has granted medRxiv a license to display the preprint in perpetuity. It is made available under a CC-BY-NC-ND 4.0 International license .

diagnosis of H1N1 with microfluidic convection PCR. Microsyst Technol. Springer Berlin Heidelberg; 2017;23: 2951–2956. doi:10.1007/s00542-016-2979-z

36. Nguyen T, Duong Bang D, Wolff A. 2019 Novel Coronavirus Disease (COVID-19): Paving the Road for Rapid Detection and Point-of-Care Diagnostics. Micromachines. MDPI AG; 2020;11: 306. doi:10.3390/mi11030306

37. Udugama B, Kadhiresan P, Kozlowski HN, Malekjahani A, Osborne M, Li VYC, et al. Diagnosing COVID-19: The Disease and Tools for Detection. ACS Nano. American Chemical Society; 2020; doi:10.1021/acsnano.0c02624

38. Gates B. Responding to Covid-19 — A Once-in-a-Century Pandemic? N Engl J Med. Massachusetts Medical Society; 2020; doi:10.1056/nejmp2003762

39. Yu L, Wu S, Hao X, Li X, Liu X, Ye S, et al. Rapid colorimetric detection of COVID-19 coronavirus using a reverse tran-scriptional loop-mediated isothermal amplification (RT-LAMP) diagnostic plat-form: iLACO. medRxiv. Cold Spring Harbor Laboratory Press; 2020; 2020.02.20.20025874. doi:10.1101/2020.02.20.20025874

40. Zhang Y, Odiwuor N, Xiong J, Sun L, Nyaruaba RO, Wei H, et al. Rapid Molecular Detection of SARS-CoV-2 (COVID-19) Virus RNA Using Colorimetric LAMP. medRxiv. Cold Spring Harbor Laboratory Press; 2020;2: 2020.02.26.20028373. doi:10.1101/2020.02.26.20028373

41. Park G-S, Ku K, Beak S-H, Kim SJ, Kim S Il, Kim B-T, et al. Development of Reverse Transcription Loop-mediated Isothermal Amplification (RT-LAMP) Assays Targeting SARS-CoV-2. bioRxiv. Cold Spring Harbor Laboratory; 2020; 2020.03.09.983064. doi:10.1101/2020.03.09.983064

42. Zhu X, Wang X, Han L, Chen T, Wang L, Li H, et al. Reverse transcription loop-

medRxiv preprint doi: https://doi.org/10.1101/2020.04.09.20058651; this version posted April 14, 2020. The copyright holder for this preprint (which was not certified by peer review) is the author/funder, who has granted medRxiv a license to display the preprint in perpetuity. It is made available under a CC-BY-NC-ND 4.0 International license .

mediated isothermal amplification combined with nanoparticles-based biosensor for diagnosis of COVID-19. medRxiv. Cold Spring Harbor Laboratory Press; 2020; 2020.03.17.20037796. doi:10.1101/2020.03.17.20037796

43. Lamb LE, Bartolone SN, Ward E, Chancellor MB. Rapid Detection of Novel Coronavirus (COVID19) by Reverse Transcription-Loop-Mediated Isothermal Amplification. SSRN Electron J. Elsevier BV; 2020; doi:10.2139/ssrn.3539654

44. Jiang M, Fang W, Aratehfar A, Li X, ling L, Fang H, et al. Development and validation of a rapid single-step reverse transcriptase loop-mediated isothermal amplification (RT-LAMP) system potentially to be used for reliable and high-throughput screening of COVID-19. medRxiv. Cold Spring Harbor Laboratory Press; 2020; 2020.03.15.20036376. doi:10.1101/2020.03.15.20036376

45. Santiago GT De, Gante CR De, García-Lara S, Ballescá-Estrada A, Alvarez MM. Studying mixing in Non-Newtonian blue maize flour suspensions using color analysis. PLoS One. Public Library of Science; 2014;9. doi:10.1371/journal.pone.0112954

46. OSF Preprints | Landscape Coronavirus Disease 2019 test (COVID-19 test) in vitro -- A comparison of PCR vs Immunoassay vs Crispr-Based test [Internet]. [cited 8 Apr 2020]. Available: https://osf.io/6eagn

47. Tanner NA, Zhang Y, Evans TC. Visual detection of isothermal nucleic acid amplification using pH-sensitive dyes. Biotechniques. Eaton Publishing Company; 2015;58: 59–68. doi:10.2144/000114253

48. Rusk N. Torrents of sequence. Nature Methods. Nature Publishing Group; 2011. p. 44. doi:10.1038/nmeth.f.330

49. Wang W, Xu Y, Gao R, Lu R, Han K, Wu G, et al. Detection of SARS-CoV-2 in

medRxiv preprint doi: https://doi.org/10.1101/2020.04.09.20058651; this version posted April 14, 2020. The copyright holder for this preprint (which was not certified by peer review) is the author/funder, who has granted medRxiv a license to display the preprint in perpetuity. It is made available under a CC-BY-NC-ND 4.0 International license .

Different Types of Clinical Specimens. JAMA - Journal of the American Medical Association. American Medical Association; 2020. doi:10.1001/jama.2020.3786

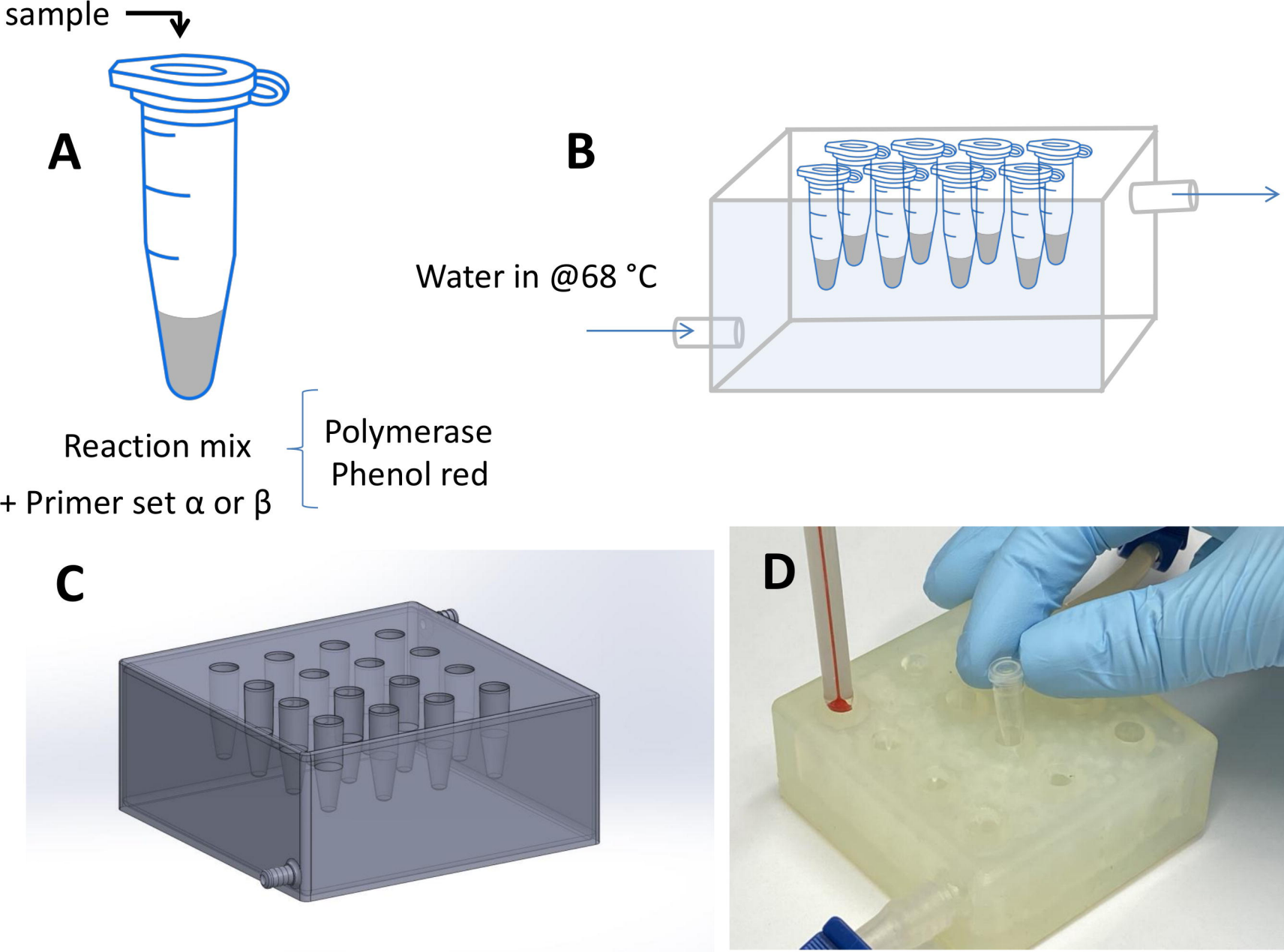
sample
A
B
Water in @68 °C
Reaction mix
+ Primer set α or β
Polymerase
Phenol red
C
D

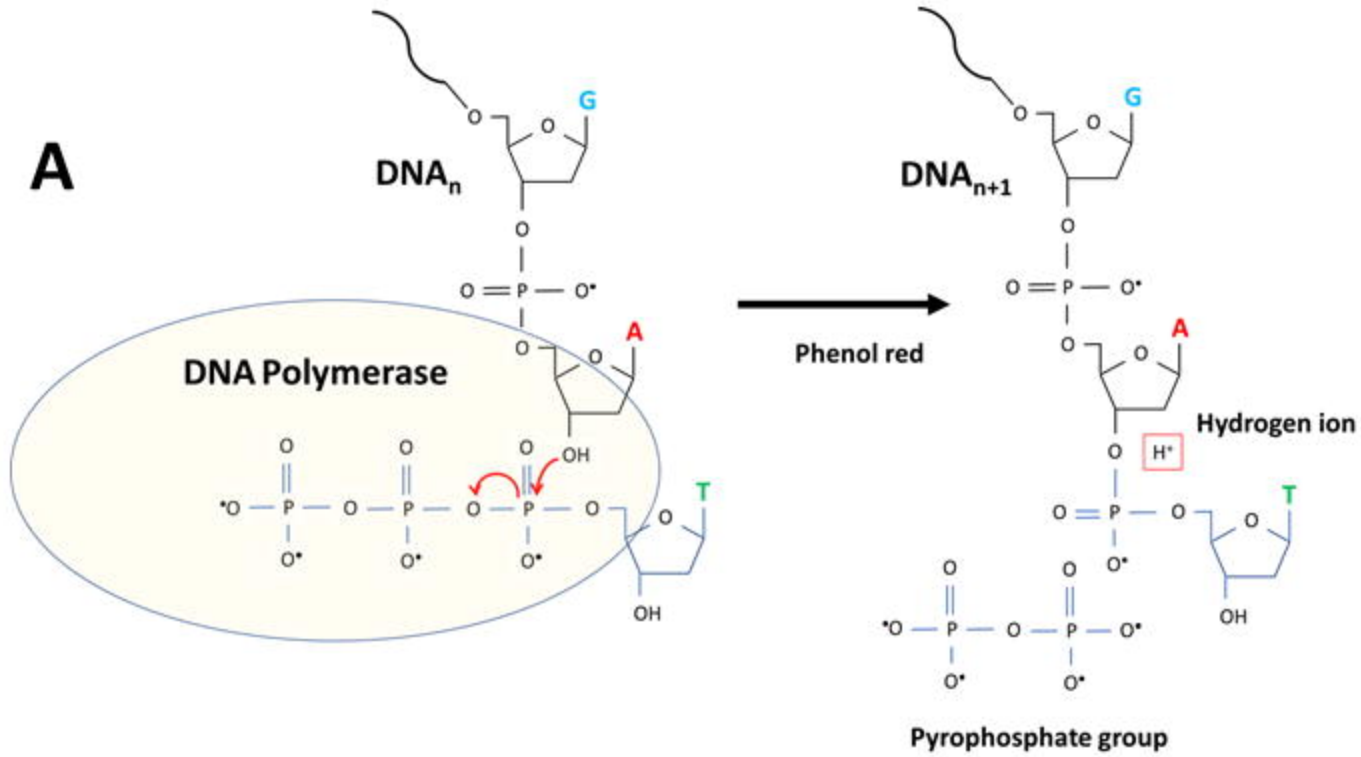
A
DNA$_n$
DNA$_{n+1}$
DNA Polymerase
Phenol red
Hydrogen ion
Pyrophosphate group
G
A
T
OH
H+

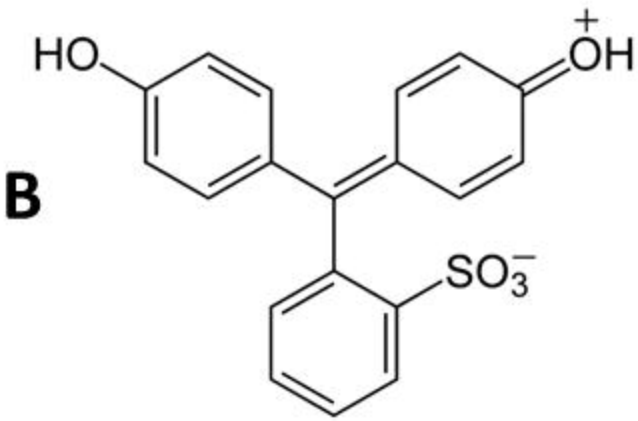
B
HO
OH
SO$_3^-$

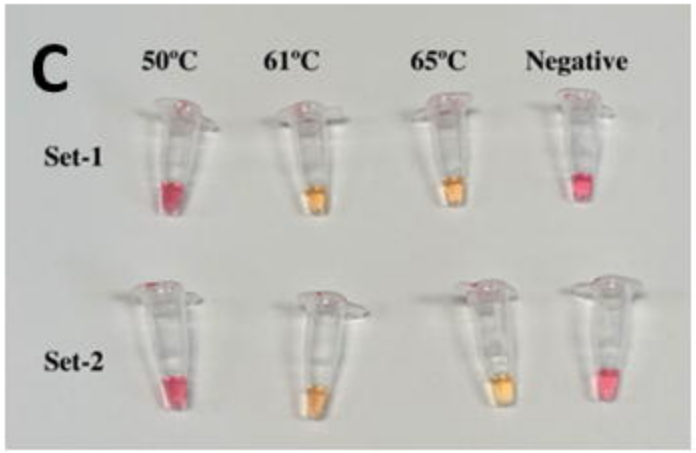
C
50°C
61°C
65°C
Negative
Set-1
Set-2

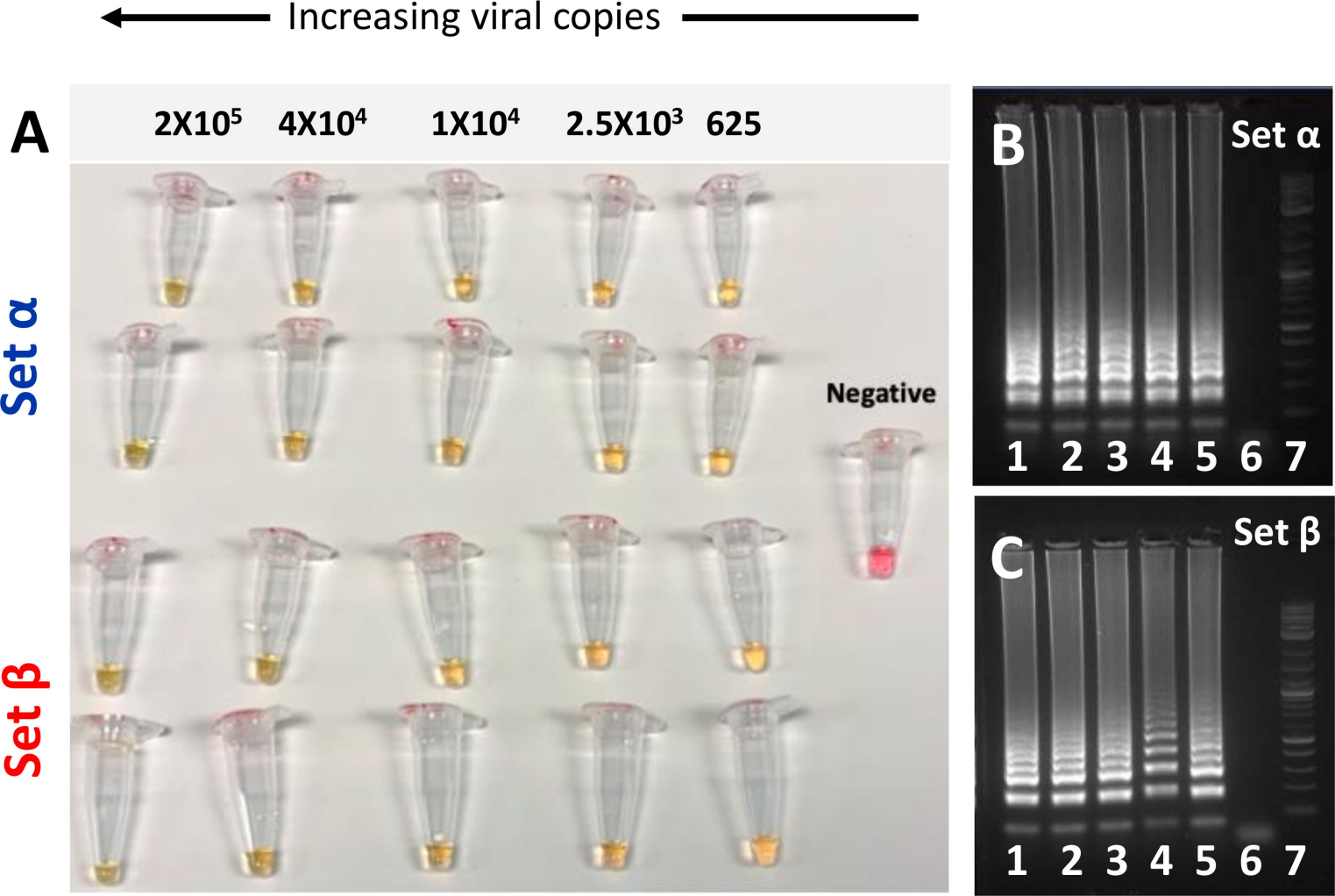
Increasing viral copies
A
2X10^5
4X10^4
1X10^4
2.5X10^3
625
Set α
Set β
Negative
B
Set α
1 2 3 4 5 6 7
C
Set β
1 2 3 4 5 6 7

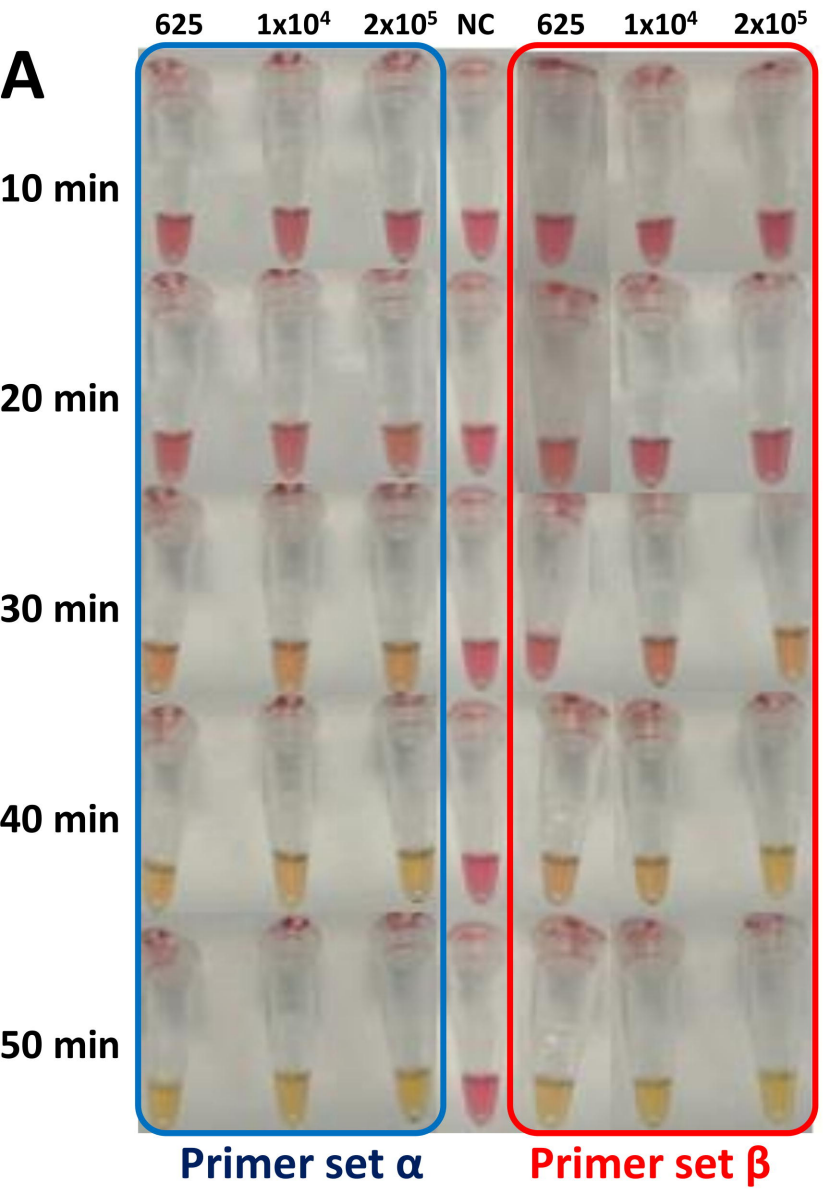
A
625
1x10⁴
2x10⁵
NC
625
1x10⁴
2x10⁵
10 min
20 min
30 min
40 min
50 min
Primer set α
Primer set β

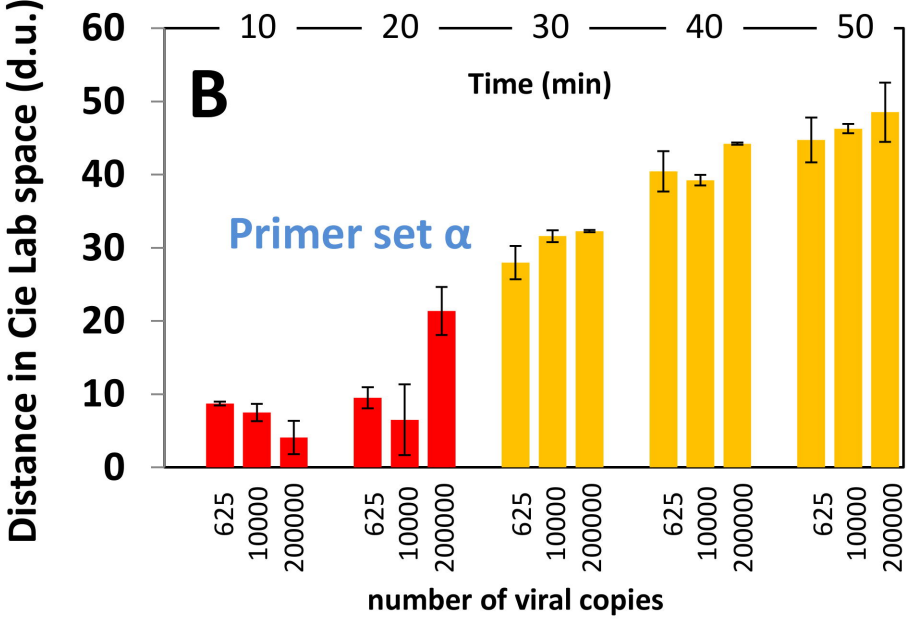
B
Time (min)
10
20
30
40
50
Primer set α
Distance in Cie Lab space (d.u.)
0
10
20
30
40
50
60
625
10000
200000
number of viral copies

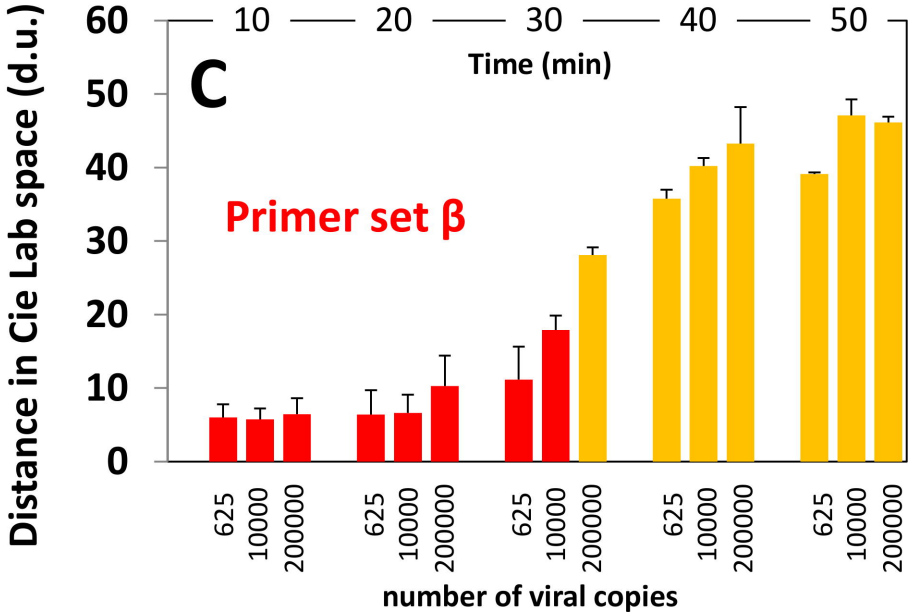
C
Time (min)
10
20
30
40
50
Primer set β
Distance in Cie Lab space (d.u.)
0
10
20
30
40
50
60
625
10000
200000
number of viral copies

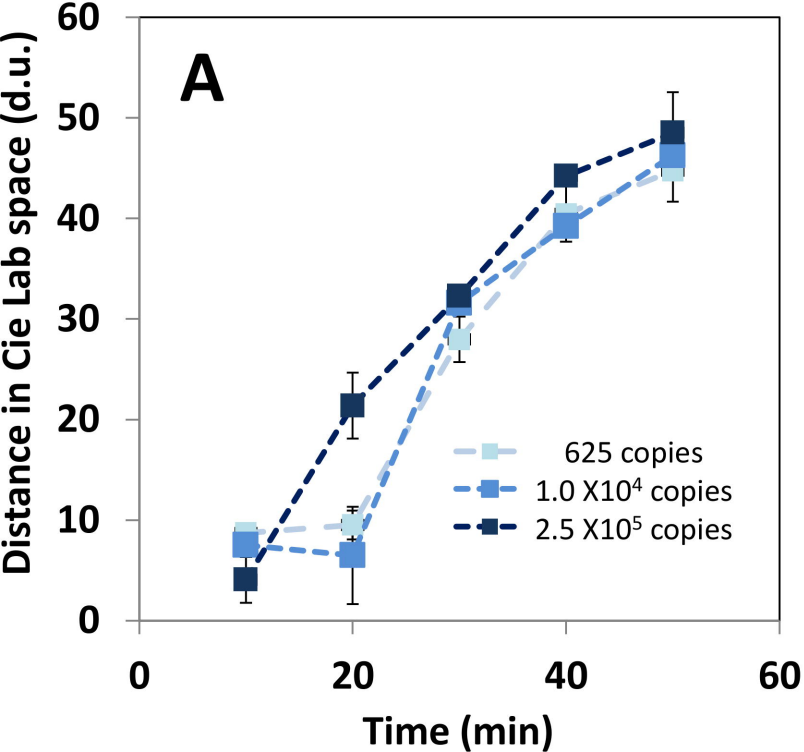
A
Distance in Cie Lab space (d.u.)
Time (min)
625 copies
1.0 X10^4 copies
2.5 X10^5 copies
0
10
20
30
40
50
60
0
20
40
60

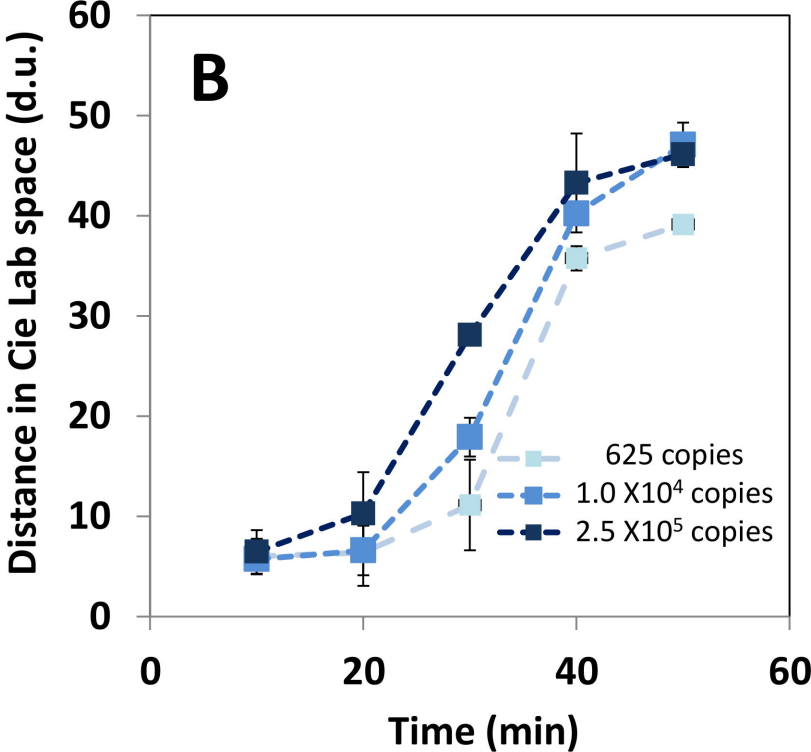
B
Distance in Cie Lab space (d.u.)
Time (min)
625 copies
1.0 X10^4 copies
2.5 X10^5 copies
0
10
20
30
40
50
60
0
20
40
60